

TNF Induced Switching of Columnar Rectangular to Hexagonal Assemblies in a New Class of Triphenylene-Based Room Temperature Discotic Liquid Crystals

Monika Gupta, Santosh Prasad Gupta, and Santanu Kumar Pal

J. Phys. Chem. B, **Just Accepted Manuscript** • DOI: 10.1021/acs.jpcc.7b06737 • Publication Date (Web): 17 Aug 2017

Downloaded from <http://pubs.acs.org> on August 19, 2017

Just Accepted

“Just Accepted” manuscripts have been peer-reviewed and accepted for publication. They are posted online prior to technical editing, formatting for publication and author proofing. The American Chemical Society provides “Just Accepted” as a free service to the research community to expedite the dissemination of scientific material as soon as possible after acceptance. “Just Accepted” manuscripts appear in full in PDF format accompanied by an HTML abstract. “Just Accepted” manuscripts have been fully peer reviewed, but should not be considered the official version of record. They are accessible to all readers and citable by the Digital Object Identifier (DOI®). “Just Accepted” is an optional service offered to authors. Therefore, the “Just Accepted” Web site may not include all articles that will be published in the journal. After a manuscript is technically edited and formatted, it will be removed from the “Just Accepted” Web site and published as an ASAP article. Note that technical editing may introduce minor changes to the manuscript text and/or graphics which could affect content, and all legal disclaimers and ethical guidelines that apply to the journal pertain. ACS cannot be held responsible for errors or consequences arising from the use of information contained in these “Just Accepted” manuscripts.



1
2
3
4
5
6 TNF Induced Switching of Columnar Rectangular
7
8
9
10 to Hexagonal Assemblies in a New Class of
11
12
13
14 Triphenylene-Based Room Temperature Discotic
15
16
17
18
19 Liquid Crystals
20
21
22

23
24 *Monika Gupta, Santosh Prasad Gupta, and Santanu Kumar Pal**
25

26
27 Department of Chemical Sciences, Indian Institute of Science Education and Research
28
29 (IISER) Mohali, Sector-81, Knowledge City, Manauli-140306, India
30
31

32
33 **ABSTRACT.** A straightforward synthesis of triphenylene-based oligomeric systems that
34
35 self-organize into room temperature columnar structures is presented. The compounds with
36
37 longer spacer length ($m = 10$ and 12) exhibit columnar rectangular (Col_r) mesophase whereas
38
39 the compound with $m = 8$ exists in glassy Col_r state. Interestingly, the Col_r self-assembly of
40
41 these compounds switches to columnar hexagonal (Col_h) on doping the compounds with 2, 4,
42
43 7-trinitrofluorenone (TNF). For the dopant concentration of 1:1 with respect to native
44
45 compound, an intermediate transition state between Col_r and Col_h phase was observed which
46
47 completely transformed into the hexagonal phase on increasing the concentration to 1:2
48
49 (compound: TNF) and afterwards. Both the Col_r and Col_h self-assemblies have been well
50
51 resolved by detailed X-ray analysis. These kind of oligomeric compounds generally possess a
52
53 combination of desirable alignment properties analogous to monomeric compounds and long-
54
55 lived glassy states similar to that of polymeric mesogens. In addition, charge hopping
56
57
58
59
60

1

behaviour is expected to increase in these compounds due to donor-acceptor interactions. Overall, these compounds can find possible potential applications in semiconductor devices.

1. INTRODUCTION

Recently, there has been substantial interest in the field of non-conventional low molar mass discotic liquid crystals (LCs) *i.e.* dimers and oligomers because of their fascinating mesomorphic properties due to restricted molecular motions.¹⁻⁴ These discotic LC oligomers serve as ideal illustrative compounds for polymers due to ease of purification & characterisation and remarkable similarities in their transitional behaviour.⁵ The physical properties of these discotic LC oligomers are also notably different from their constituent units. They are more prone to form columnar glasses which are mechanically stiff and have potential applications as the anisotropic properties of mesophase and macroscopic alignment of domains is vitrified and the columnar ordering is preserved in these systems.⁶⁻⁸ Therefore, oligomeric discogens possess the combination of desirable alignment properties of monomers with the long-lived glassy state of the polymers.

Till date, triphenylene (TP) is the most widely studied scaffold in the family of discotic LCs and thus its derivatives are ideal workhorses for analysing the properties of discotic LC oligomers and polymers as TP is easy to obtain in both mono as well as bifunctional forms.⁹⁻¹¹ Triphenylene oligomers have drawn particular attention as they show improved optical and electronic properties.¹²⁻²⁰ They are generally constructed by grafting triphenylenes onto various functional frameworks. Most workers have concentrated on linear & star-shaped oligomers containing three mesogenic moieties. However, fewer examples of star-shaped oligomers containing four mesogenic moieties connected to a common nucleus have been reported so far. The reported examples mainly include the triphenylene tetramers with

1
2
3 siloxane core, spirocarbon spacer, triazole bridges, rigid aromatic Schiff-bases and hydrogen-
4
5 bonding spacers.²¹⁻²⁶ All these tetramers displayed excellent LC properties with lower phase
6
7 transition temperatures.
8

9
10 In this report, we have designed new star-shaped oligomeric mesogens in which
11
12 azobenzene was chosen as rigid core attached to which are four TP units *via* varying flexible
13
14 alkyl spacers. LCs comprising photo-responsive moieties such as azobenzene have been
15
16 established as promising materials for applications in photomechanics, instant displays,
17
18 reversible holographic storage and digital storage due to their high resolution and
19
20 sensitivity.²⁷⁻²⁹ Therefore, azobenzene will not only act as a linker for the triphenylene cores
21
22 but can also impart interesting properties to these oligomers due to its photoresponsive
23
24 behaviour. The oligomers synthesised in this study were found to self-assemble in a columnar
25
26 rectangular fashion at room-temperature. We have further introduced 2, 4, 7-
27
28 trinitrofluorenone (TNF) in the columnar assemblies of these oligomers. TNF which is an
29
30 electron-acceptor moiety can form charge transfer (CT) interactions which can induce,
31
32 stabilize as well as extend the mesomorphic range of the native compound.³⁰⁻³³ Not only this,
33
34 it can also improve the charge carrier mobilities by facilitating charge transfer and thus
35
36 preventing recombination. In this process, intermediate excited charge-transfer (CT) states
37
38 are formed where the holes are present on the donor and electron at the acceptor molecule.
39
40 Thus, on applying electric field the electrical conductivity rises due to an increase in charge
41
42 migration.³⁴⁻³⁷ Oligomeric mesogens generally possess higher values of charge carrier
43
44 mobilities due to larger delocalisation of π -electrons and thus a lower band gap. Further,
45
46 introducing TNF in these kind of oligomeric systems can lead to an increment in the charge
47
48 carrier mobilities. Therefore, the CT complexes of these oligomeric systems containing four
49
50 TP connected to an azobenzene core will be interesting from the device point of view.
51
52
53
54
55
56
57
58
59
60

1
2
3 Surprisingly, we have found for the first time that columnar rectangular (Col_r) self-assembly
4
5 of these oligomers at room-temperature switches to columnar hexagonal (Col_h) fashion on
6
7 doping the compounds with TNF. The combination of the various properties such as LC
8
9 phase at room-temperature, easy alignment by mechanical shearing, increased charge
10
11 hopping expected from the donor-acceptor charge transfer complexes and switching from
12
13 columnar rectangular to hexagonal phase makes these oligomers very advantageous for new
14
15 device applications.
16
17

18 19 **2. EXPERIMENTAL SECTION**

20 21 **2.1 Materials and Reagents**

22
23
24
25
26 Chemicals and solvents were all of AR quality and were used without further purification.
27
28 Catechol, bromohexane, ferric chloride, 2-bromo-1,3,2-benzodioxaborole, cesium carbonate,
29
30 dibromooctane, dibromodecane, dibromododecane, potassium iodide, 5-nitroisophthalic acid,
31
32 sodium hydroxide, potassium hydroxide, dextrose, hydrochloric acid, n-butanone and
33
34 tetraoctyl ammonium bromide were all purchased from Sigma–Aldrich (Bangalore, India).
35
36 Column chromatographic separations were performed on silica gel (60-120 & 230-400
37
38 mesh). Thin layer chromatography (TLC) was performed on aluminium sheets pre-coated
39
40 with silica gel (Merck, Kieselgel 60, F254).
41
42

43 44 **2.2 Instrumental**

45
46
47 **Structural characterization.** Structural characterization of the compound was carried out
48
49 through a combination of infrared spectroscopy (Perkin Elmer Spectrum AX3), ^1H NMR and
50
51 ^{13}C NMR (Bruker Biospin Switzerland Avance-iii 400 MHz and 100 MHz spectrometers
52
53 respectively) and UV-VIS-NIR spectrophotometer (Agilent Technologies UV-vis-NIR
54
55
56
57
58
59
60

Spectrophotometer). NMR spectra were recorded using deuterated chloroform (CDCl_3) as solvent and tetramethylsilane (TMS) as an internal standard.

Differential Scanning Calorimetry. DSC measurements were performed on Perkin Elmer DSC 8000 coupled to a Controlled Liquid Nitrogen Accessory (CLN 2) with a scan rate of 5 $^{\circ}\text{C}/\text{min}$.

Polarized Optical Microscopy. Textural observations of the mesophase were performed with Nikon Eclipse LV100POL polarising microscope provided with a Linkam heating stage (LTS 420). All images were captured using a Q-imaging camera.

X-ray Diffraction. X-ray diffraction (XRD) was carried out on powder samples using $\text{Cu K}\alpha$ ($\lambda=1.54 \text{ \AA}$) radiation from a source (GeniX 3D, Xenocs) operating at 50 kV and 0.6 mA. The diffraction patterns were collected on a two module Pilatus detector.

2.3 Synthesis of oligomers 7

Synthesis of compounds **2**, **3**, **4** and **6** has been described in the earlier reports (Scheme 1).³⁸⁻⁴² For the synthesis of the target compound **7**, compound **6** (1 equivalent) was dissolved in aqueous KOH (1.1 equivalent) solution. To that solution, compound **4** (6 equivalents) was added followed by the addition of tetraoctylammonium bromide in catalytic amounts. The reaction mixture was refluxed under vigorous stirring for 5 hours & was then cooled to room temperature. The compound was extracted with dichloromethane. The organic layer was washed with brine & dried over anhydrous sodium sulphate. The chloroform was removed by rotary evaporation and the resulting residue was purified by column chromatography over silica gel using hexane & ethyl acetate as eluent. The synthesized compounds **7a-c** were characterized by ^1H NMR, ^{13}C NMR, IR, UV-vis and elemental analysis as shown below:

Compound 7a

^1H NMR (400 MHz, CDCl_3 , δ in ppm): 8.81 (t, 2H, $J = 1.6$ Hz), 8.77 (d, 4H, $J = 1.6$ Hz), 7.84 (s, 24H), 4.42 (t, 8H, $J = 4, 8$ Hz), 4.24 (m, 48H), 1.92 (m, 56H), 1.52 (m, 152H), 0.95 (m, 60H).

^{13}C NMR (400 MHz, CDCl_3 , δ in ppm): 165.24, 152.27, 148.96, 148.95, 148.90, 132.17, 123.60, 123.57, 107.33, 107.25, 69.70, 69.67, 69.61, 65.91, 31.72, 29.54, 29.47, 29.45, 29.35, 28.73, 26.20, 25.97, 25.88, 22.70, 14.10.

FT-IR (cm^{-1}): 3090.94, 2929.95, 2858.29, 1726.46, 1616.88, 1514.87, 1468.88, 1435.28, 1388.50, 1310.41, 1261.99, 1234.89, 1170.40, 1104.75, 1042.01, 923.59, 867.74, 837.26, 802.35, 758.78, 726.87, 684.06, 600.61.

UV-vis (nm): 251, 262, 270, 280, 309, 346, 444.

Elemental analysis (%): Calculated C 76.27 H 9.44 N 0.74. Found C 76.34 H 9.51 N 1.09.

Compound 7b

^1H NMR (400 MHz, CDCl_3 , δ in ppm): 8.82 (s, 2H), 8.79 (s, 4H), 7.84 (s, 24H), 4.41 (t, 8H, $J = 8$ Hz), 4.24 (t, 8H, $J = 8$ Hz), 1.95 (m, 48H), 1.85 (m, 8H), 1.59 (m, 40H), 1.41 (m, 128H), 0.95 (m, 60 H).

^{13}C NMR (400 MHz, CDCl_3 , δ in ppm): 165.23, 148.95, 148.92, 123.58, 107.29, 69.69, 31.71, 29.66, 29.58, 29.54, 29.45, 29.37, 28.73, 26.25, 26.00, 25.87, 22.88, 14.10, 14.08.

FT-IR (cm^{-1}): 3096.6, 2929.47, 2857.75, 1726.35, 1616.93, 1514.77, 1468.61, 1435.52, 1388.47, 1310.23, 1262.48, 1235.31, 1170.73, 1042.42, 923.77, 867.46, 837.10, 802.68, 758.82, 726.10, 683.92, 600.68.

UV-vis (nm): 251, 261, 270, 280, 308, 346, 443.

Elemental analysis (%): Calculated C 76.54 H 9.58 N 0.72. Found C 76.16 H 9.61 N 0.99.

Compound 7c

¹H NMR (400 MHz, CDCl₃, δ in ppm): 8.84 (t, 2H, *J* = 2, 1.2 Hz), 8.80 (d, 4H, *J* = 1.6 Hz), 7.85 (s, 24H), 4.42 (t, 8H, *J* = 4, 8 Hz), 4.25 (t, 48H, *J* = 8 Hz), 1.96 (m, 48H), 1.85 (m, 8H), 1.60 (m, 40H), 1.40 (m, 144H), 0.96 (m, 60H).

¹³C NMR (400 MHz, CDCl₃, δ in ppm): 165.27, 152.32, 148.95, 148.94, 132.24, 127.90, 123.59, 107.27, 69.68, 65.98, 31.73, 29.74, 29.71, 29.63, 29.54, 29.46, 29.38, 28.73, 26.26, 26.01, 25.89, 22.70, 14.11.

FT-IR (cm⁻¹): 3100.3, 2926.32, 2855.88, 1726.58, 1615.40, 1515.54, 1469.16, 1434.76, 1389.7, 1314.5, 1264.4, 1234.79, 1170.57, 1046.2, 925.23, 869.62, 840.18, 800.93, 761.68, 722.43, 683.18, 604.68.

UV-vis (nm): 251, 261, 270, 280, 309, 346, 443.

Elemental analysis (%): Calculated C 76.80 H 9.72 N 0.70. Found C 76.62 H 9.76 N 0.97.

2.4 Preparation of CT complexes. The amount of TNF and oligomer was calculated according to molar ratios. The calculated amount was dissolved in dichloromethane and both the solutions were mixed. The resulting solution which was of deep brown colour was then allowed to evaporate by leaving the solution to stand overnight. The final traces of solvent were removed under high vacuum.

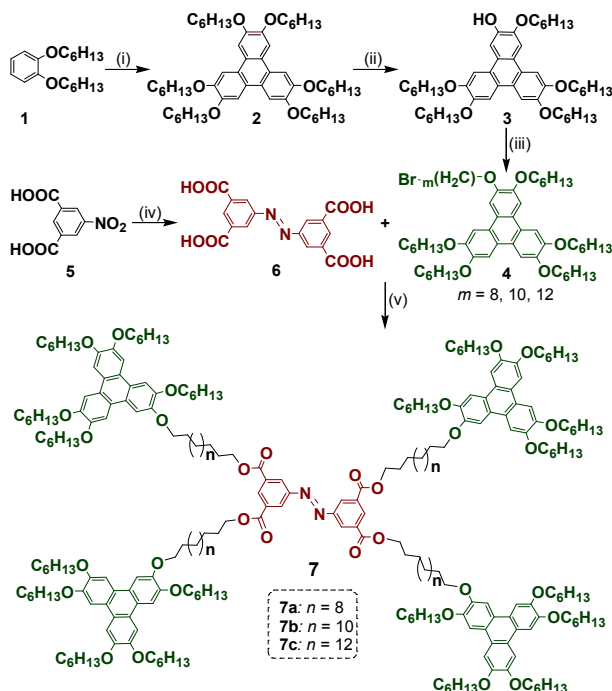
3. RESULTS AND DISCUSSION

Synthesis and structural characterization

The target compounds were obtained by following the synthetic route as illustrated in Scheme 1. Synthesis of compounds **2**, **3**, **4** and **6** has been described in the earlier reports.³⁸⁻⁴²

The final compounds **7** were prepared by reacting the triphenylene derivative **4** and azobenzene tetracarboxylic acid **6** in presence of potassium hydroxide and tetraoctylammonium bromide using water as solvent under reflux for around 7 hours (see

experimental section for details). All the compounds were characterised by ^1H NMR, ^{13}C NMR, IR, UV-vis and elemental analysis (ESI, Figure S1-S8).

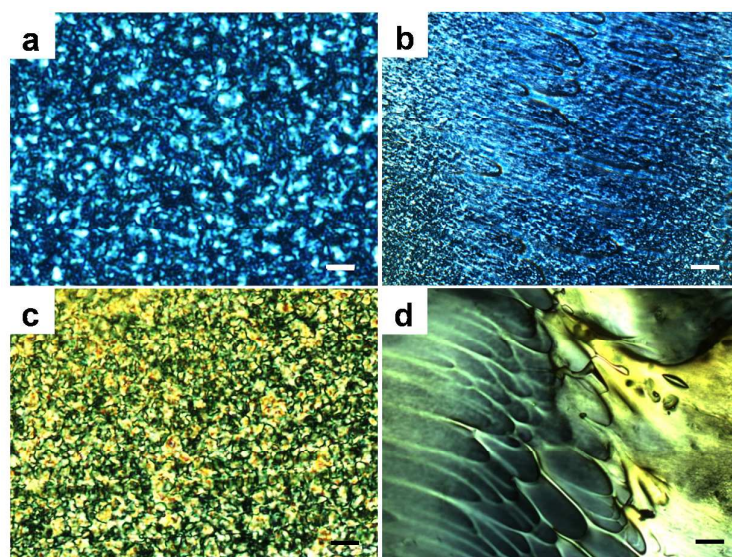


Scheme 1. Synthesis of the target compounds **7**. Reagents and conditions: (i) FeCl_3 , CH_2Cl_2 , H_2SO_4 , RT, 1 h, 70%; (ii) Cat-B-Br, CH_2Cl_2 , RT, 48 h, 40%; (iii) CS_2CO_3 , KI, butanone, 80 $^\circ\text{C}$, 18 h, 85%; (iv) NaOH, dextrose, 80 $^\circ\text{C}$, HCl, 70%; (v) KOH, H_2O , TOAB, reflux, 5h, 50%.

Thermal Behavior

Thermal behavior of all the compounds was investigated with the help of Polarizing Optical Microscopy (POM) and Differential Scanning Calorimetry (DSC). Compound **7a** was a transparent glassy material and displayed a glass to isotropic transition at 77 $^\circ\text{C}$ on heating, whereas, on cooling it remained isotropic till room temperature. For compounds **7b** and **7c**, the presence of thermotropic LC phase at room temperature was confirmed with the highly birefringent textures and their shearability under polarizing optical microscopy (POM)

1
2
3 observation (Figure 1). Compounds **7b** & **7c** exhibited isotropization at 40.3 °C & 43.5 °C
4
5 respectively. However, on further cooling, the mesophase did not appear immediately till
6
7 room temperature (ESI, Figure S9). This was a general observation for all the compounds and
8
9 the mesophase only reappears after keeping the isotropic melt for few hours. A possible
10
11 explanation for this behaviour could be that the triphenylene molecules are connected *via*
12
13 relatively short spacers to a rigid core and do not have enough freedom in a short time span to
14
15 self-assemble into columns on subsequent cooling from isotropic state.
16
17
18
19



38
39
40
41
42
43
44
45
46
47
48
49
50
51
52
53
54
55
56
57
58
59
60

Figure 1. Optical photomicrograph of compound (a) **7b** and (c) **7c** obtained with a polarized optical microscope at 25 °C (crossed polarizers, magnification $\times 50$). (b) & (d) represent the respective textures after shearing the film. (scale bar = 10 μm).

To further explore mesophase behaviour of the synthesized compounds SAXS/WAXS experiments were carried out. As concluded from POM observations, compounds **7b** & **7c** were showing LC behaviour at room temperature whereas compound **7a** was glassy in nature. However, in XRD studies it was found that diffractograms of all the three compounds were similar (Figure 2). This indicates that the self-assembly of molecules in **7a** is similar to that in **7b** and **7c**, however, the motion of alkyl chains is frozen in **7a**. In-order to find out the

detailed structure of the assembly of compound **7**, we have carried out a thorough analysis on diffractogram of compound **7c**. This analysis could explain the structure of assembly of compound **7b** and **7a**, because the diffraction pattern for both of them are similar to **7c**.

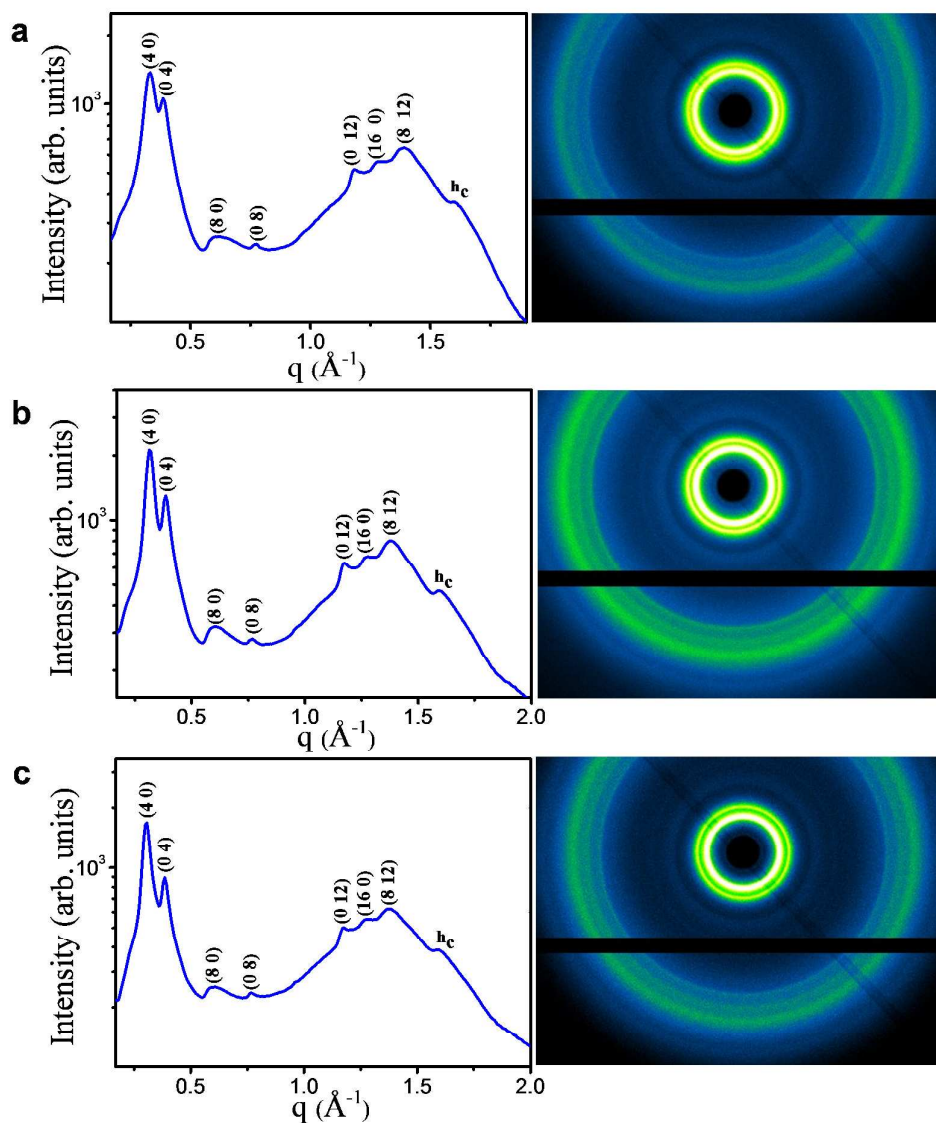


Figure 2. X-ray diffraction pattern corresponding to mesophases of compound (a) **7a**, (b) **7b** and (c) **7c** indexed on columnar rectangular (Col_r) phase. Right panel shows the respective 2D diffraction patterns.

1
2
3 The diffraction pattern of compound **7c** exhibits many peaks as shown in Figure 2. In
4 particular, it showed h_c peak of spacing of about 3.93 Å in the wide angle region which
5 appears due to π - π interaction and correspond to face to face separation between TP groups.
6
7 Hence, it confirms the columnar nature of the structure of assembly of compound **7c** and
8 indicates that TP cores are assembled on top of each other to form columns which are further
9 arranged on a 2D lattice. This h_c peak gives the value of one of the lattice parameter, *i.e.*, $c =$
10 3.93 Å. However, the reported face-to-face distance between two π -conjugated molecules is
11 in the range of 3.5-3.7 Å which suggests that the TP cores are packed with a tilting angle of
12 23.37 ± 3.69 degrees with respect to the columnar axis. The XRD pattern further exhibit four
13 peaks in the small angle region. Interestingly, the d -spacing of the first and third peak as well
14 as that of second and fourth peak are in the ratio of 1:1/2, indicating the lamellar nature of the
15 structure in two different directions. We have also performed the SAXS experiment at lower
16 q region but could not see any additional peak in that region which could be assigned to
17 lower hk values (Figure S10). In-order to understand the detailed arrangement of columns on
18 2D lattice and to facilitate their indexing, GIWAXS/SAXS experiments were also carried out
19 on oriented thin films obtained through mechanical shearing on an ITO coated glass substrate
20 (Figure 3). The GISAXS pattern of the sample showed partially aligned peaks in the small
21 angle region (Figure 3a). Azimuthal plot of the first two peaks of the small angle shows that
22 they are orthogonal to each-other (Figure 3b). Further, each of the first two peaks is two-fold
23 confirming that the structure is rectangular.
24
25
26
27
28
29
30
31
32
33
34
35
36
37
38
39
40
41
42
43
44
45
46
47

48 Therefore, combining the information from SAXS/WAXS and GISAXS, it is clear that TP
49 cores massed on top of each other and form columns and the arrangement of columns on 2D
50 lattice exhibit lamellar ordering in two orthogonal directions in the columnar plane. Based on
51
52
53
54
55
56
57
58
59
60

above analysis, a possible model representing the self-assembly in compounds **7** is shown in Figure 4.

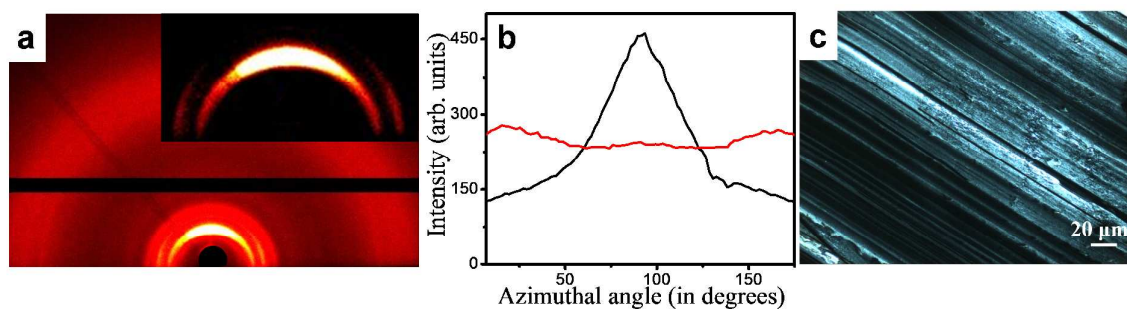


Figure 3. (a) GIWAXS & GISAXS (inset) pattern from a thin oriented film obtained through mechanical shearing of compound **7c** on ITO coated glass substrate. (b) Azimuthal plot of the first two peaks, (40) and (04). Both peaks are orthogonal to each other and each one is two-fold in nature. (c) Optical micrograph of the oriented film of compound **7c** as viewed between crossed polarizers.

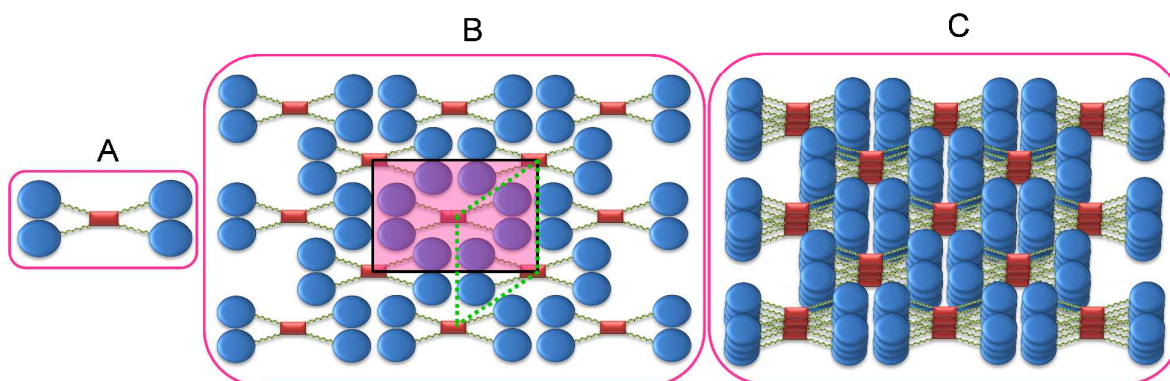


Figure 4. Schematic of (A) the structure of compound **7**, modelled as four triphenyl (TP) discs (in blue colour) connected with azobenzene group (in red color) *via* flexible spacers. (B) A possible arrangement of columns on 2D rectangular lattice where centre of azo group forms a rectangular lattice. Box in the black colour show the unit cell of rectangular lattice. (C) A possible arrangement of columns on 2D rectangular lattice where centre of azo group forms a rectangular lattice.

1
2
3 Addition of TNF to compound **7**, transforms the rectangular lattice into hexagonal lattice.
4
5 Green dotted parallelogram with modified dimensions represents the unit cell of hexagonal
6
7 lattice. (C) 3D arrangement of structure representing the columnar rectangular (Col_r) phase.
8
9

10
11 The compounds **7** are discotic mesogenic quadric based on TP linked with azobenzene
12
13 group via flexible alkyl spacers. The compound could be modelled as four TP discs (blue in
14
15 colour) tethered *via* flexible alkyl chains to an azobenzene group (red in colour). The model
16
17 shows that the centre of the azo group forms the rectangular lattice (Figure 4). The rectangle
18
19 with black boundary shows the unit cell of the lattice. The unit cell also exhibits the lamellar
20
21 of the column layers in two orthogonal directions as suggested by SAXS/WAXS and
22
23 GISAXS analysis (Figure 5). The lamellar periodicity is $a/4$ and $b/4$ in two orthogonal
24
25 directions of rectangle, respectively, indicating that the indexes of first two peaks would be
26
27 (40) and (04) and also suggests that the allowed reflection would be $h, k = 4n$ (Figure 5a).
28
29 Other reflection of un-oriented pattern is indexed accordingly and structure of the assembly is
30
31 Col_r. The d -spacing are calculated according to equation $1/d_{cal}^2 = h^2/a^2 + k^2/b^2$ where h
32
33 and k are the miller indices. The calculated lattice parameters are $a = 81.28 \text{ \AA}$ and $b = 65.20$
34
35 \AA . The details are summarized in the Table 1. This assignment of hk values was done to
36
37 represent the actual symmetry of the molecular arrangement. The present indexing indicates
38
39 that the unit cell has four-fold lamellar ordering of the column layer with periodicities $a/4$ and
40
41 $b/4$ along the direction of a and b , respectively. This is consistent with most possible
42
43 arrangement of the molecule in the rectangular (Col_r) phase (Figure 4) and also the symmetry
44
45 of the unit cell of Col_r phase (Figure 5a). Deducing the hk values to lower numbers (*i.e.* 10
46
47 and 01) will lead to lattice dimensions of about $1/4^{\text{th}}$ of the present value and will correspond
48
49 to about one TP unit of the oligomer. The symmetry of unit cell and its arrangement in the
50
51 rectangular lattice cannot be justified in that case.
52
53
54
55
56
57
58
59
60

Table 1. The observed and calculated d -spacings and planes, correlation length of the diffraction peaks of the columnar rectangular (Col_r) phase observed in compound **7c** with the lattice parameters: $a = 81.28 \text{ \AA}$, $b = 65.20 \text{ \AA}$ and $c = 3.93 \text{ \AA}$. d_{exp} is the observed d -spacing. d_{cal} is the calculated d -spacing according to formula $\frac{1}{d_{\text{cal}}^2} = \frac{h^2}{a^2} + \frac{k^2}{b^2}$. ξ is the correlation length.

Planes (hkl)	d -spacing d_{exp} (Å)	d -spacing d_{cal} (Å)	ξ	ξ/d_{exp}
4 0	20.32	20.32	124.27	6.11
0 4	16.30	16.30	111.84	6.86
8 0	10.25	10.16		
0 8	8.18	8.15		
12 0	6.53	6.77		
0 12	5.40	5.43		
16 0	4.95	5.08		
8 12	4.57	4.79		
h_c	3.93		23.23	5.91

The correlation length (ξ) which provides an indication of ordering within the mesophases was calculated using $\xi = [k 2\pi]/[(\Delta q)]$; equivalent to Scherrer's equation. Here, k is the shape factor whose typical value is 0.89, λ is the wavelength of the incident X-ray, q is the scattering vector ($q = 4\pi \sin\theta/\lambda$), θ is the maximum of the reflection and Δq is the broadening in q at half of the maximum intensity. The Δq is calculated from the fitting of the diffraction peaks by Lorentzian profiles. Ratio of the ξ and corresponding d -spacings gives a realization of correlation length in terms of correlated units of length scale d . The calculated correlation lengths along the a and b axis of the rectangular lattice *i.e.* corresponding to (40) and (04) peaks are 124.27 Å and 111.84 Å respectively. The corresponding number of correlated columns are about 6 and 7, respectively. The calculated core-core correlation length corresponding to h_c peak along the column (c) axis is 23.23 Å which is equivalent to about 6 correlated cores (Table 1).

As mentioned earlier, the diffraction patterns of compounds **7b** and **7a** are very similar to **7c** and explained similarly (ESI Table S1, S2). Interestingly, the lattice parameter 'a' was found to be less than **7c** in **7b** and even lesser than **7b** in compound **7a** which is obvious because spacer length in **7a** is shorter than **7b** which is further smaller than **7c**. However, the lattice parameters, *b* and *c* remain constant in compounds **7a** and **7b**. The correlation lengths corresponding to (40) and (04) peaks were found to decrease in **7b** and **7a** from its values in **7c**. The corresponding values are 101.67 Å (5 correlated columns) and 93.20 Å (about 6 correlated columns), respectively in case of compound **7b** and 78.76 Å (about 4 correlated columns) and 69.03 Å (about 4 correlated columns) for compound **7a**. Increase in correlation length along *a* and *b* direction from **7a** to **7c** attributes to the stabilization of the rectangular phase with increasing spacer length. Although, the core-core correlation length remains the same in compound **7a-c**.

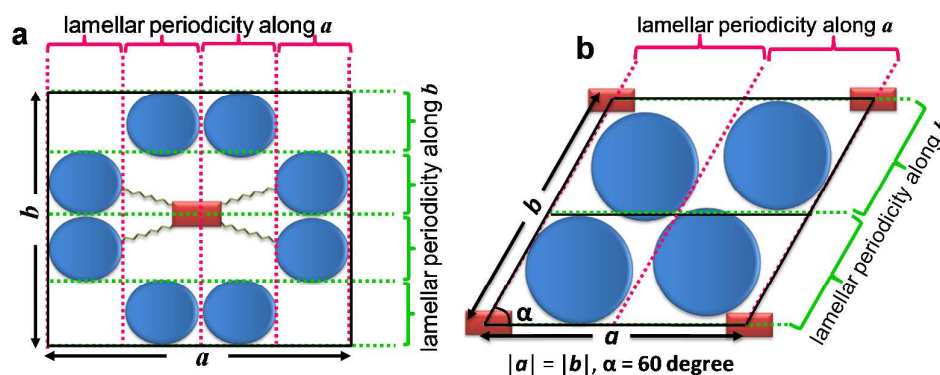
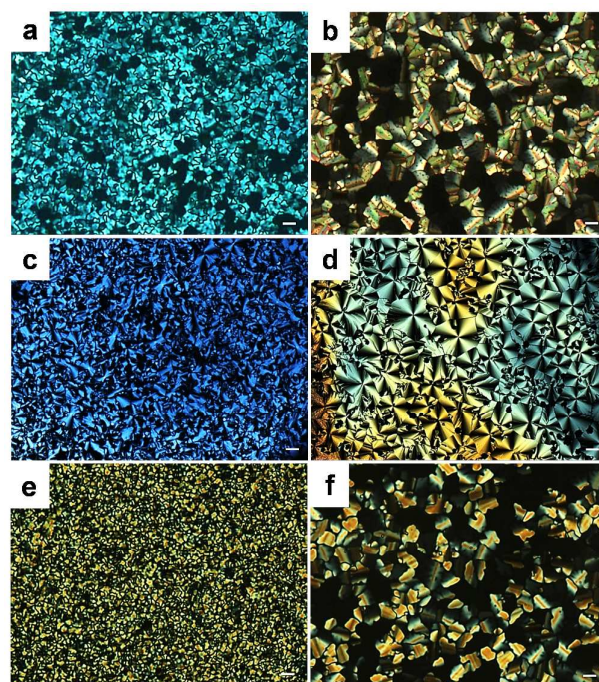


Figure 5. A schematic of unit cell of (a) columnar rectangular (Col_r) phase and (b) columnar hexagonal (Col_h) phase. Rectangular and hexagonal unit cell exhibit the lamellar of the column layers. The lamellar periodicities are $a/4$ and $b/4$ along the direction of a and b , respectively of the Col_r phase. The lamellar periodicity is $a/2$ along both the direction of Col_h phase.

Charge-transfer complexes

1
2
3 CT complexes of synthesized compounds **7** were prepared with TNF in the molar proportions
4 of 1:1, 1:2, 1:3 and 1:4 [oligomer: TNF] respectively (see experimental section for details).
5
6 Interestingly, all the complexes displayed enantiotropic LC phase behaviour at room
7 temperature which was confirmed from characteristic birefringent textures with shearability
8 of the compound at room temperature. On cooling from the isotropic phase, these complexes
9 displayed focal conic textures typical of a columnar mesophase (Figure 6, ESI Figure S11).
10
11 The precise transition temperatures and associated enthalpy changes for all the complexes are
12 listed in Table 2 (see ESI, Figure S12). It was found that the doping resulted in mesophase
13 induction for the complexes of compound **7a** which was a glassy columnar in its pure state.
14
15 Also, clearing temperatures of all the complexes increased drastically as compared to that of
16 the undoped compounds.
17
18
19
20
21
22
23
24
25
26
27



51
52 **Figure 6.** Optical photomicrographs of the doped compounds (a) **7a**: TNF [1:1] at 30.4 °C,
53 (b) **7a**: TNF [1:2] at 121.3 °C, (c) **7b**: TNF [1:1] at 45.6 °C, (d) **7b**: TNF [1:2] at 65.2 °C, (e)
54
55

1
2
3 **7c**: TNF [1:1] at 54 °C and (f) **7c**: TNF [1:2] at 100.2 °C as obtained on cooling from
4 isotropic through a polarized optical microscope with crossed polarizers (scale bar = 20 μm).
5
6
7

8 To confirm the mesophases and also for quantitative comparison, we have carried out
9 XRD studies on these complexes. Surprisingly, the mesophase switched from rectangular in
10 case of pure compounds to hexagonal phase in case of CT complexes as evident from XRD
11 studies (*vide infra*). 1:1 complexes displayed an intermediate phase between columnar
12 rectangular and hexagonal states and were completely transformed into columnar hexagonal
13 (Col_h) in case of 1:2 complexes. Moreover, 1:2 CT complexes of all the compounds were
14 found to be most stable as their clearing temperatures were highest compared to other
15 complexes (Table 2).
16
17
18
19
20
21
22
23
24
25
26
27
28
29

30 **Table 2.** Thermal behaviour of the charge transfer complexes of compounds **7** with TNF.^{a, b, c}
31
32

Complexes	Heating Scan	Cooling Scan
7a :TNF [1:1]	Col 80 (1.28) I	I 67 Col
7a :TNF [1:2]	Col _h 135.7 (3.40) I	I 125.2 (6.16) Col _h
7a :TNF [1:3]	Col _h 134.5 (3.15) I	I 121.9 (4.98) Col _h
7a :TNF [1:4]	Col _h 118.9 (1.26) I	I 111.32 (2.20) Col _h
7b :TNF [1:1]	Col 100 I	I 83 Col
7b :TNF [1:2]	Col _h 136.9 (0.41) I	I 109 (1.28) Col _h
7b :TNF [1:3]	Col _h 132.6 (0.68) I	I 117 Col _h
7b :TNF [1:4]	Col _h 130 I	I 119 Col _h
7c :TNF [1:1]	Col 100 I	I 70 Col
7c :TNF [1:2]	Col _h 121.6(2.23) I	I 103.4 (3.32) Col _h

7c:TNF [1:3]	Col _h 118.3(1.64) I	I 99.63 (2.35) Col _h
7c:TNF [1:4]	Col _h 91.98(0.51) I	I 86 (0.55) Col _h

^[a] Phase transition temperatures in °C and transition enthalpies in kJ mol⁻¹ (in parentheses).

^[b] Phase assignments: Col = Columnar, Col_h = Columnar hexagonal, I = isotropic.

^[c] For some of the complexes, transitions were not observed in DSC, however it was confirmed from POM & XRD studies.

We present here a detailed analysis on CT complexes of compound **7c**. The CT complexes of compounds **7a** & **7b** show similar behaviour to that of **7c**. Addition of TNF to compound **7c** leads to a stable Col_h phase. However, for the molar ratio (**7c**:TNF) 1:1 it exhibits a mixed phase which transformed into a stable Col_h phase for the molar ratio 1:2 and is retained for ratios 1:3 and 1:4 (Figure 7). The observation of two peaks in the small angle region with *d*-spacing in ratios of 1:1/√3 confirms a 2D hexagonal phase and h_c peak in the wide-angle region indicates the columnar nature of the structure. Thus, the addition of TNF to compound **7c** leads to changes in the structure of assembly and Col_r phase is transformed into Col_h phase. In-order to get the most possible indexing of the hexagonal phase, the unit cell is derived from the model of the rectangular lattice as shown in Figure 5b. The unit cell exhibits the lamellar ordering of the column layers along the two directions of hexagonal lattice with the periodicity *a*/2 which suggest that the allowed reflection would be *h*, *k* = 2*n*. Hence, the indexes of the first two peaks of small angle region are (20) and (22) respectively. The lattice parameter, *a* is calculated by using the relation $a = 4 d_{20}/\sqrt{3}$. The calculated value of the lattice parameter, *a* is 43.42 Å for the complex **7c**: TNF = 1:2 and h_c peak gives the value of other lattice parameter *i.e.* *c* = 3.74 Å. Further, one broad peak, h_a of spacing 4.85 Å was also found in wide angle region which is mainly originated due to alkyl chain-chain correlation

(Figure 8, Table 3). The lattice parameter, a (column-column separation) as well as c (core-core separation) is found to decrease with increasing molar ratio of TNF (Table 4).

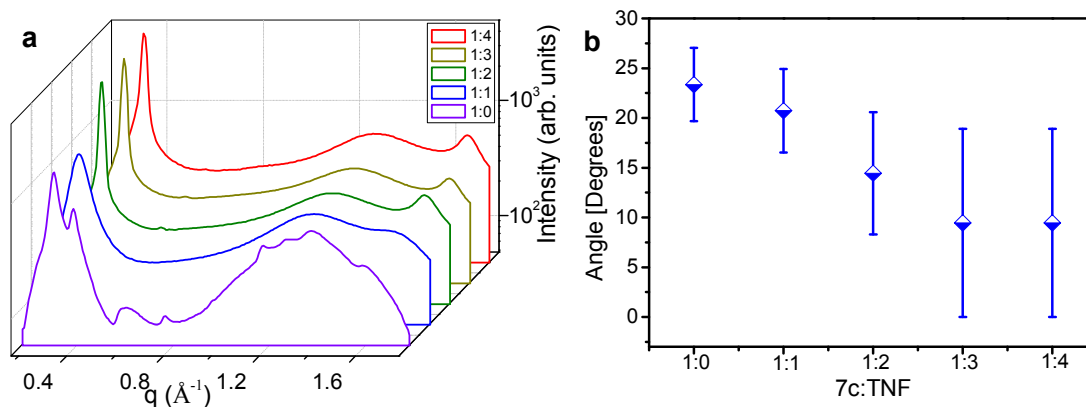


Figure 7. (a) X-ray diffraction pattern of compound $[7c: \text{TNF}] = 1:0$ to $1:4$ which describes the changeover of columnar rectangular (Col_r) phase into columnar hexagonal (Col_h) phase on increasing the TNF concentration. (b) Variation of tilt angle (of the TP cores in column with respect column axis) with increasing concentration of TNF along with error bar.

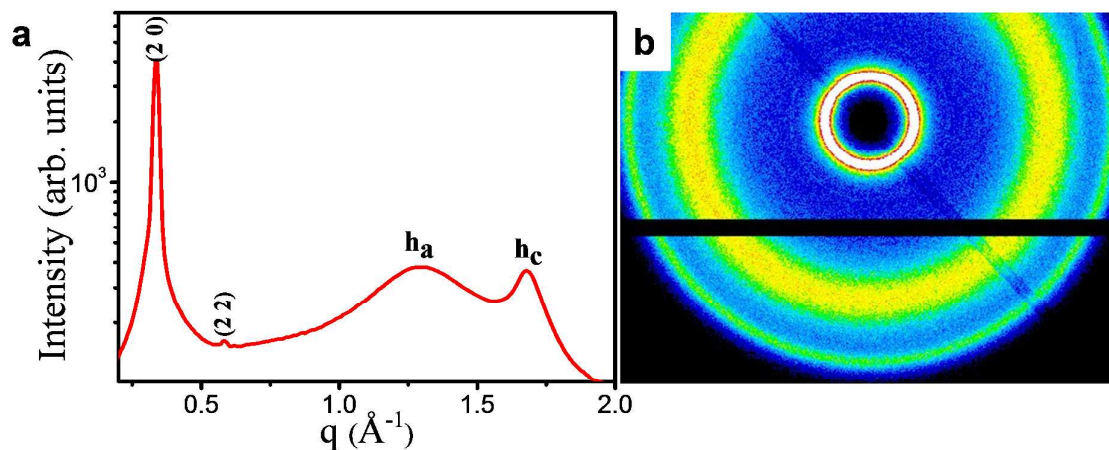


Figure 8. (a) X-ray diffraction pattern of compound $7c: \text{TNF} = 1:2$ with indexing on the columnar hexagonal (Col_h) phase. (b) Corresponding 2D diffraction pattern in the mesophase.

Table 3. The observed and calculated d -spacings and planes, correlation length of the diffraction peaks of the columnar hexagonal (Col_h) phase observed in compound $7c: \text{TNF} =$

1:2 with the lattice parameters: $a = 43.42 \text{ \AA}$ and $c = 3.74 \text{ \AA}$. d_{exp} is the observed d -spacing.

d_{cal} is the calculated d -spacing according to formula: $\frac{1}{d_{\text{cal}}^2} = \frac{4}{3} \left(\frac{h^2 + hk + k^2}{a^2} \right)$ for hexagonal phase. ξ is the correlation length.

Planes (hkl)	d -spacing d_{exp} (Å)	d -spacing d_{cal} (Å)	ξ	ξ/d_{exp}
2 0	18.80	18.80	223.68	11.89
2 2	10.78	10.86		
h_a	4.85			
h_c	3.74		43.01	11.57

The calculated column-column correlation length corresponding to (20) peak is $\sim 224 \text{ \AA}$ for complex **7c**: TNF = 1:2 which is equivalent to about 12 correlated columns. The calculated core-core correlation length was found to be approximately $\sim 43 \text{ \AA}$, corresponding to about 11 correlated cores which is double of the value as observed in the pure compound **7c**. The number of correlated cores remains same with increasing molar ratio of TNF (Table 4). Interestingly, addition of TNF to compound **7c** reduces the tilting angle of TP core with respect to the columnar axis from 23.37 ± 3.69 degrees to 9.45 ± 9.45 degrees and helps to relax the TP cores in columns leading to the transformation from Col_r to Col_h phase (Figure 7). Effect of introducing TNF in the compounds **7a** and **7b** is very similar to that of **7c** and can be explained similarly (ESI, Figure S13-15, Table S3 and S4).

A thorough literature survey revealed that there are two possible ways in which TNF can be accommodated in the columnar assembly.³⁰⁻³⁷ One of them is side by side manner and the other is in intercalated fashion. We believe that our study supports that TNF molecules are more likely to be present in an intercalated fashion rather than side by side manner which is based on the following facts: 1) Tilt angle of columns with respect to columnar axis in compound **7** exhibiting Col_r phase decreases on transformation to Col_h phase on introducing

1
2
3 TNF. Further, tilt angle decreases with increasing molar ratio of TNF. 2) The calculated
4 intercolumnar and intracolumnar correlation lengths in the Col_h phase were found to be
5 approximately double of the values observed for Col_r phase, confirming that the addition of
6 TNF into compound 7 significantly increases the ordering in the system. Further, the
7 calculated volume of the unit cell of Col_r lattice is about 20,826 Å³ (for compound 7c) which
8 contains about two oligomers (Figure 5a). However, the calculated volume of the unit cell of
9 Col_h lattice is about 6,106 Å³ (for compound 7c: TNF = 1:2) which accommodates nearly one
10 oligomeric unit (Figure 5b). Therefore, the available volume per molecule in the Col_h phase is
11 significantly less in comparison to Col_r phase which indicates that the TNF molecule will
12 most likely not arrange in the side by side fashion, due to lack of enough gap between column
13 to accommodate TNF molecules. Further, the probability of TNF molecules being present in
14 the fluid chain matrix can also be ignored because that will randomise the system and hence
15 reduce the correlation length which is in direct conflict with our experimental observations.
16 Hence, TNF molecules are most possibly arranged in the intercalated manner. Further, TNF
17 molecule can form a charge complexion with TP moiety, thus leading to an increased
18 ordering along the column axis which was indeed observed in our studies. Charge
19 complexion also relaxes the column and reduces the tilt angle which helps the columns to be
20 more symmetric and arrange on 2D hexagonal lattice with significant planar ordering as seen.
21 All these observations support an intercalated arrangement of TNF molecules.
22
23
24
25
26
27
28
29
30
31
32
33
34
35
36
37
38
39
40
41
42
43
44
45
46
47
48
49
50
51
52
53
54
55
56
57
58
59
60

Table 4. Variation of different observed and calculated lattice parameters and corresponding correlation lengths for compounds **7** and their mixtures with TNF.

a

Compound/ Mixtures	7a	7a :TNF [1:1]	7a :TNF [1:2]	7a :TNF [1:3]	7a :TNF [1:4]
Phase	Col _r	Mixed	Col _h	Col _h	Col _h
Lattice parameter: 2D (a, b) &	(77.28, 65.20)	--	40.34	40.22	39.58
Column-Column correlation	(78.76, 69.03)	--	223.68	223.68	199.71
No. Of correlated columns	(4.09, 4.23)		12.80	12.84	11.65
Core-Core correlation length (Å)	23.23	29.43	43.01	46.60	46.60
No. Of correlated cores	5.23	7.68	11.50	12.60	12.53

b

Compound/ Mixtures	7b	7b :TNF [1:1]	7b :TNF [1:2]	7b :TNF [1:3]	7b :TNF [1:4]
Phase	Col _r	Mixed	Col _h	Col _h	Col _h
Lattice parameter: 2D (a, b) &	(80.26, 65.20)	--	41.90	41.52	40.60
Column-Column correlation	(101.67, 93.20)	--	223.68	223.68	199.71
No. Of correlated columns	(5.06, 5.72)		12.33	12.44	11.65
Core-Core correlation length (Å)	23.23	29.43	43.01	46.60	46.60
No. Of correlated cores	5.91	7.68	11.57	12.53	12.53

c

Compound/ Mixtures	7c	7c :TNF [1:1]	7c :TNF [1:2]	7c :TNF [1:3]	7c :TNF [1:4]
Phase	Col _r	Mixed	Col _h	Col _h	Col _h
Lattice parameter: 2D (a, b) &	(81.28, 65.20)	--	21.71	20.95	21.05
Column-Column correlation	(124.27, 111.84)	--	223.68	223.68	199.71
No. Of correlated columns	(6.11, 6.86)		11.89	12.33	10.95
Core-Core correlation length (Å)	23.23	26.62	43.01	46.60	46.60
No. Of correlated cores	5.91	7.68	11.57	12.53	12.53

Photophysical & Electrochemical studies

For the estimation of electrical band gap, electrochemical behaviour of compound **7c** was studied by cyclic voltammetry of 0.001 M solution in 0.1 M of tetrabutylammonium perchlorate (TBAP) as a supporting electrolyte in dry dichloromethane (Figure 9).⁴³ For these studies, a 0.1 M solution of tetrabutylammonium hexafluorophosphate was used as supporting electrolyte in dichloromethane. A single compartment cell fitted with Ag/AgNO₃

1
2
3 reference electrode, platinum wire counter electrode and glassy carbon working electrode was
4
5 used for experiment. The reference electrode was calibrated with the ferrocene/ferrocenium
6
7 (Fc/Fc⁺) redox couple (absolute energy level of 4.80 eV to vacuum, see ESI, section-8). The
8
9 cyclic voltammogram was recorded with a scanning rate of 0.1 V/s. Compound **7c** displayed
10
11 reversible oxidation and reduction curves as indicated from its anodic and cathodic peak
12
13 potential responses. The HOMO and LUMO energy levels were calculated using the formula:

$$E_{\text{HOMO}} = - (E_{\text{oxd,onset}} - E_{1/2, \text{Fc, Fc}^+} + 4.8) \text{ eV}$$

$$E_{\text{LUMO}} = - (E_{\text{red,onset}} - E_{1/2, \text{Fc, Fc}^+} + 4.8) \text{ eV}$$

14
15
16
17
18
19
20
21
22
23
24 The band gap was estimated using the relation:

$$\Delta E_g = E_{\text{HOMO}} - E_{\text{LUMO}}$$

25
26
27
28
29
30 The HOMO and LUMO energy levels were estimated to be -5.82 and -2.62 eV, respectively.
31
32 The electrical band gap was calculated to be 3.20 eV. The optical band gap calculated from
33
34 the red edge of the absorption spectra for compounds **7** was around 2.30 eV which is much
35
36 lesser as compared to electrical band gap.
37

38
39
40 We did not observe any photoisomerization effects due to azobenzene core in these oligomers
41
42 even in very dilute solutions. This effect is in contrast to the earlier reported examples where
43
44 the azobenzene core was connected to relatively flexible units. *e.g.* azobenzene
45
46 tetracarboxylic core when connected to benzene or 1, 3, 4-oxadiazole units through various
47
48 linkages, displayed trans to cis conversion on irradiation with UV light and subsequent
49
50 conversion from cis to trans on irradiation with visible light.^{44, 45} The absence of
51
52 photoisomerization effects in the present oligomers could be ascribed to the restricted rotation
53
54
55
56
57
58
59
60

of the photo-responsive azobenzene core as it is tethered to four bulkier triphenylene units which provides more steric restriction as compared to the benzene and 1,3,4-oxadiazole units.

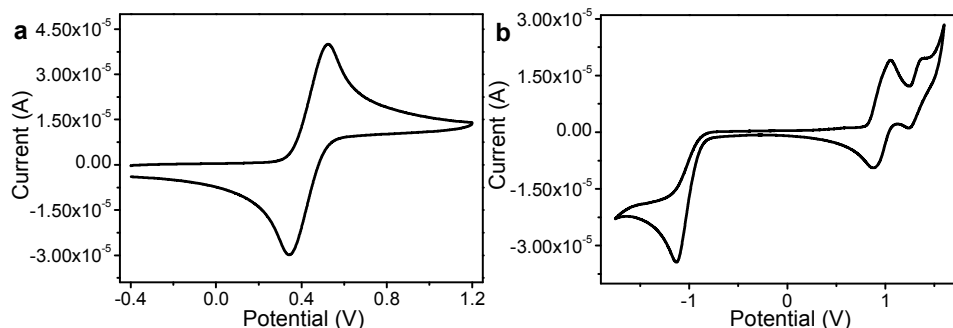


Figure 9. (a) Cyclic voltammogram of ferrocene in anhydrous dichloromethane solution of tetrabutylammonium hexafluorophosphate (0.1 M). (b) Cyclic voltammogram of compound 7c in anhydrous dichloromethane solution of tetrabutylammonium hexafluorophosphate (0.1 M) at a scanning rate of 0.5 mV/s.

CONCLUSIONS

Triphenylene-based oligomeric LCs in which TP units were connected to an azobenzene core have been synthesized and characterized using well known characterization techniques. The compounds with spacer length $m = 10, 12$ exhibited LC properties even at room temperature as confirmed from POM and XRD studies. Compounds with spacer lengths of $m = 8$ displayed a columnar glassy state. Interestingly, the transition from Col_r to Col_h phase was observed on introducing the TNF moiety into columnar self-assemblies of these compounds. These kind of oligomeric LCs generally possess intermediate properties between that of the monomeric LCs and those of the polymeric LCs. In addition, the observation of mesophase at room temperature and increased charge hopping arising from the donor-acceptor charge transfer complexes makes them very useful for device application. We have also

demonstrated the methodology to control self-assembly of columnar mesophase which could be advantageous for certain device applications.

ASSOCIATED CONTENT

Supporting Information

^1H and ^{13}C NMR, UV-vis and IR spectra of the synthesized oligomers, DSC thermogram, 2D X-ray diffraction patterns and details of cyclic voltammetry. This material is available free of charge via the Internet at <http://pubs.acs.org>.

AUTHOR INFORMATION

Corresponding Author

*Corresponding author: Tel.: +91-172-2240266; fax: +91-172-2240266; E-mail: skpal@iisermohali.ac.in and santanupal.20@gmail.com

Notes

The authors declare no competing financial interest.

ACKNOWLEDGEMENT

We are thankful to NMR and SAXS/WAXS facility at IISER Mohali. Dr. SK Pal is grateful for financial support from INSA (bearing sanction No. SP/YSP/124/2015/433). M. Gupta acknowledges the receipt of a graduate fellowship from IISER Mohali. We thank Mr. Vaibhav Pal for experimental support.

REFERENCES

- 1
2
3 (1) Imrie, C. T.; Henderson, P. A. Liquid Crystal Dimers and Higher Oligomers: Between
4 Monomers and Polymers. *Chem. Soc. Rev.* **2007**, *36*, 2096-2124.
5
6
7
8 (2) Kumar, S. Self-Organization of Disc-Like Molecules: Chemical Aspects. *Chem. Soc. Rev.*
9 **2006**, *35*, 83-109.
10
11
12 (3) Wöhrle, T.; Wurzbach, I.; Kirres, J.; Kostidou, A.; Kapernaum, N.; Litterscheidt, J.;
14 Haenle, J. C.; Staffeld, P.; Baro, A.; Giesselmann, F.; et al. Discotic Liquid Crystals. *Chem.*
16 *Rev.* **2016**, *116*, 1139-1241.
17
18
19 (4) Sergeyeve, S.; Pisula, W.; Geerts, Y. H. Discotic Liquid Crystals: A New Generation of
21 Organic Semiconductors. [Chem. Soc. Rev.](#) **2007**, *36*, 1902-1929.
22
23
24 (5) Kranig, W.; Hueser, B.; Spiess, H. W.; Kreuder, W.; Ringsdorf, H.; Zimmermann, H.
26 Phase Behavior of Discotic Liquid Crystalline Polymers and Related Model Compounds.
28 *Adv. Mater.* **1990**, *2*, 36-40.
29
30
31 (6) Boden, N.; Bushby, R. J.; Cammidge, A. N.; Mansoury, A. E.; Martin, P. S.; Lu, Z. The
33 Creation of Long-Lasting Glassy Columnar Discotic Liquid Crystals Using 'Dimeric'
35 Discogens. *J. Mater Chem.* **1999**, *9*, 1391-1402.
36
37
38 (7) Boden, N.; Bushby, R. J.; Lu, Z. A Rational Synthesis of Polyacrylates with Discogenic
40 Side Groups. *Liq. Cryst.* **1998**, *25*, 47-58.
41
42
43 (8) Boden, N.; Bushby, R. J.; Cammidge, A. N.; Martin, P. S. Glass-forming Discotic Liquid-
45 Crystalline Oligomers. *J. Mater. Chem.* **1995**, *5*, 1857-1860.
46
47
48 (9) Kumar, S. Recent Developments in the Chemistry of Triphenylene-Based Discotic Liquid
50 Crystals. *Liq. Cryst.* **2004**, *31*, 1037-1059.
51
52
53
54
55
56
57
58
59
60

- 1
2
3 (10) Kumar, S. Triphenylene-Based Discotic Liquid Crystal Dimers, Oligomers and
4 Polymers. *Liq. Cryst.* **2005**, *32*, 1089–1113.
5
6
7
8 (11) Pal, S. K.; Setia, S.; Avinash, B. S.; Kumar, S. Triphenylene-Based Discotic Liquid
9 Crystals: Recent Advances. *Liq. Cryst.* **2013**, *40*, 1769–1816.
10
11
12
13 (12) Adam, D.; Schuhmacher, P.; Simmerer, J.; Häussling, L.; Siemensmeyer, K.; Etzbach,
14 K. H.; Ringsdorf, H.; Haarer, D. Fast Photoconduction in the Highly Ordered Columnar
15 Phase of a Discotic Liquid Crystal. *Nature* **1994**, *371*, 141–143.
16
17
18
19
20
21 (13) Van de Craats, A. M.; Warman, J. M.; De Haas, M. P.; Adam, D.; Simmerer, J.; Haarer,
22 D.; Schuhmacher, P. The Mobility of Charge Carriers in All Four Phases of the Columnar
23 Discotic Material Hexakis (hexylthio) Triphenylene: Combined TOF and PR-TRMC Results.
24 *Adv. Mater.* **1996**, *8*, 823–826.
25
26
27
28
29
30
31 (14) Paraschiv, I.; De Lange, K.; Giesbers, M.; Van Lagen, B.; Grozema, F. C.; Abellon, R.
32 D.; Siebbeles, L. D. A.; Eijr, S.; Zuilhof, H.; Marcelis, A. T. M. Hydrogen-Bond Stabilized
33 Columnar Discotic Benzenetrisamides with Pendant Triphenylene Groups. *J. Mater. Chem.*
34 **2008**, *18*, 5475–5481.
35
36
37
38
39
40
41 (15) Bayer, A.; Zimmermann, S.; Wendorff, J. H. Low Molar Mass and Polymer Discotics:
42 Structure, Dynamics and Opto-Electronic Properties. *Mol. Cryst. liq. Cryst.* **2003**, *396*, 1-22.
43
44
45
46 (16) Marguet, S.; Markovitsi, D.; Millie, P.; Sigal, H.; Kumar, S. Influence of Disorder on
47 Electronic Excited States: An Experimental and Numerical Study of Alkylthiotriphenylene
48 Columnar Phases. *J. Phys. Chem. B* **1998**, *102*, 4697-4710.
49
50
51
52
53
54
55
56
57
58
59
60

- 1
2
3 (17) Heppke, G.; Kruerke, D.; Lohning, C.; Lotzsch, D.; Moro, D.; Muller, M.; Sawade, H.
4
5 New Chiral Discotic Triphenylene Derivatives Exhibiting a Cholesteric Blue Phase and a
6
7 Ferroelectrically Switchable Columnar Mesophase. *J. Mater. Chem.* **2000**, *10*, 2657-2661.
8
9
- 10 (18) Ichimura, K.; Furumi, S.; Morino, S.; Kidowaki, M.; Nakagawa, M.; Ogawa, M.;
11
12 Nishiura, Y. Photocontrolled Orientation of Discotic Liquid Crystals. *Adv. Mater.* **2000**, *12*,
13
14 950-953.
15
16
17
- 18 (19) Kumar, S.; Manickam, M. Preliminary Communication First Example of a
19
20 Functionalized Triphenylene Discotic Trimer: Molecular Engineering of Advanced Materials.
21
22 *Liq. Cryst.* **1999**, *26*, 939-941.
23
24
25
- 26 (20) Paraschiv, I.; Giesbers, M.; Van Lagen, B.; Grozema, F. C.; Abellon, R. D.; Laurens, D.
27
28 A.; Siebbeles, L. D. A.; Marcelis, A. T. M.; Zuilhof, H.; Sudhölter, E. J. R. H-Bond-
29
30 Stabilized Triphenylene-Based Columnar Discotic Liquid Crystals. *Chem. Mater.* **2006**, *18*,
31
32 968-974.
33
34
35
- 36 (21) Zniber, R.; Achour, R.; Cherkaoui, M. Z.; Donnio, B.; Gehringerb, L.; Guillon, D.
37
38 Columnar Mesophase from a New Hybrid Siloxane-Triphenylene. *J. Mater. Chem.* **2002**, *12*,
39
40 2208-2213.
41
42
43
- 44 (22) Markovitsi, D.; Marguet, S.; Bondkowski, J. Triplet Excitation Transfer in Triphenylene
45
46 Columnar Phases. *J. Phys. Chem. B* **2001**, *105*, 1299-1306.
47
48
49
- 50 (23) Schulte, J. L.; Laschat, S.; Vill, V.; Nishikawa, E.; Finkelmann, H.; Nimitz, M.
51
52 Convergent Synthesis of Columnar Twins and Tetramers from Triphenylene building blocks
53
54 - The First Example of a Columnar Spiro-Twin. *Eur. J. Org. Chem.* **1998**, *32*, 2499-2506.
55
56
57
58
59
60

- 1
2
3 (24) Jiang, S.; Guo, H.; Zhu, S.; Yang, F. Novel Columnar Liquid Crystalline Oligomers:
4 Triphenylene Tetramers with Rigid Aromatic Schiff-Bases and Hydrogen-Bonding Spacers
5 via Click Chemistry. *J. Mol. Liq.* **2017**, *236*, 76–80.
6
7
8
9
10 (25) Zelcer, A.; Donnio, B.; Bourgogne, C.; Cukiernik, F. D.; Guillon, D. Mesomorphism of
11 Hybrid Siloxane-Triphenylene Star-Shaped Oligomers. *Chem. Mater.* **2007**, *17*, 1992–2006.
12
13
14
15 (26) Plesnivý, T.; Ringsdorf, H.; Schuhmacher, P.; Nuutz, U.; Diele, S. Star-Like Discotic
16 Diquid Crystals. *Liq. Cryst.* **1995**, *18*, 185–190.
17
18
19
20 (27) Matharu, A. S.; Jeeva, S.; Ramanujam, P. S. Liquid Crystals for Holographic Optical
21 Data Storage. *Chem. Soc. Rev.* **2007**, *36*, 1868–1880.
22
23
24
25 (28) Shibaev, V.; Bobrovsky, A.; Boiko, N. Photoactive Liquid Crystalline Polymer Systems
26 with Light-Controllable Structure and Optical Properties. *Prog. Polym. Sci.* **2003**, *28*, 729–
27 836.
28
29
30
31 (29) Yesodha, S. K.; Pillai, C. K. S.; Tsutsumi, N. Stable Polymeric Materials for Nonlinear
32 Optics: A Review Based on Azobenzene Systems. *Prog. Polym. Sci.* **2004**, *29*, 45–74.
33
34
35
36 (30) Ringsdorf, H.; Wustefeld, R.; Zerta, E.; Ebert, M.; Wendorff, J. H. Induction of Liquid
37 Crystalline Phases: Formation of Discotic Systems by Doping Amorphous Polymers with
38 Electron Acceptors. *Angew. Chem.* **1989**, *28*, 914-918.
39
40
41
42 (31) Ringsdorf, H.; Wustefeld, R.; Karthaus, O.; Bengs, H.; Ebert, M.; Wendorff, J. H.;
43 Praefcke, K.; Kohne, B. Induction and Variation of Discotic Columnar Phases Through
44 Doping with Electron Acceptors. *Adv. Mater.* **1990**, *2*, 141-144.
45
46
47
48
49
50
51
52
53
54
55
56
57
58
59
60

- 1
2
3 (32) Destrade, C.; Foucher, P.; Gasparoux, H.; Nguyen, H. T.; Levelut, A. M.; Malthete, J.
4
5 Disc-Like Mesogen Polymorphism. *Mol. Cryst. Liq. Cryst.* **1984**, *106*, 121-146.
6
7
8 (33) Ebert, M.; Frick, G.; Baehr, C.; Wendorff, J. H.; Wüstefeld, R.; Ringsdorf, H. Structure
9
10 Formation in Doped Discotic Polymers and Low Molar Mass Model Systems. *Liq. Cryst.*
11
12 **1992**, *11*, 293-309.
13
14
15 (34) Gupta, S. K.; Raghunathan, V. A.; Lakshminarayanan, V.; Kumar, S. Novel Benzene-
16
17 Bridged Triphenylene-Based Discotic Dyads. *J. Phys. Chem. B* **2009**, *113*, 12887-12895.
18
19
20 (35) Balagurusamy, V. S. K. Quasi-One Dimensional Electrical Conductivity and
21
22 Thermoelectric Power Studies on a Discotic Liquid Crystal. *Pramana* **1999**, *53*, 3-11.
23
24
25 (36) Donovan, K. J.; Scott, K.; Somerton, M.; Preece, J.; Manickam, M. Transient
26
27 Photocurrents in a Charge Transfer Complex of Trinitrofluorenone with a Carbazole
28
29 Substituted Discotic Liquid Crystal. *Chem. Phys.* **2006**, *322*, 471-476.
30
31
32 (37) Kruglova, O.; Mendes, E.; Yildirim, Z.; Wübbenhorst, M.; Mulder, F. M.; Stride, J. A.;
33
34 Picken, S. J.; Kearley, G. J. Structure and Dynamics of a Discotic Liquid-Crystalline Charge-
35
36 Transfer Complex. *Chem. Phys. Chem.* **2007**, *8*, 1338 – 1344.
37
38
39 (38) Gupta, M.; Agarwal, N.; Arora, A.; Kumar, S.; Kumar, B.; Sheet, G.; Pal, S. K.
40
41 Synthesis and Characterization of Novel Azobenzene-Based Mesogens and Their
42
43 Organization at the Air–Water and Air–Solid interfaces. *RSC Adv.* **2014**, *4*, 41371-41377.
44
45
46 (39) Gupta, M.; Gupta, S. P.; Mohapatra, S. S.; Dhara, S.; Pal, S. K. Room-Temperature
47
48 Oligomeric Discotic Nematic Liquid Crystals Over a Wide Temperature Range: Structure-
49
50 Property Relationships. *Chem. Eur. J.* **2017**, *23*, 10626-10631.
51
52
53
54
55
56
57
58
59
60

1
2
3 (40) Gupta, M.; Bala, I.; Pal, S. K. A Room Temperature Discotic Mesogenic Dyad Based-on
4
5 Triphenylene and Pentaalkynylbenzene. *Tetrahedron Lett.* **2014**, *55*, 5836-5840.
6
7

8 (41) Gupta, M.; Pal, S. K. Triphenylene-Based Room-Temperature Discotic Liquid Crystals:
9
10 A New Class of Blue-Light-Emitting Materials with Long-Range Columnar Self-Assembly.
11
12 *Langmuir* **2016**, *32*, 1120-1126.
13
14

15 (42) Gupta, M.; Gupta, S. P.; Rasna, M. V.; Adhikari, D.; Dhara, S.; Pal, S. K. A New
16
17 Strategy Towards the Synthesis of a Room-Temperature Discotic Nematic Liquid Crystal
18
19 Employing Triphenylene and Pentaalkynylbenzene Units. *Chem. Commun.* **2017**, *53*, 3014-
20
21 3017.
22
23
24

25 (43) Kirres, J.; Schmitt, K.; Wurzbach, I.; Giesselmann, F.; Ludwigs, S.; Ringenberg, M.;
26
27 Ruff, A.; Baro, A.; Laschat, S. Tuning Liquid Crystalline Phase Behaviour in Columnar
28
29 Crown Ethers by Sulfur Substituents. *Org. Chem. Front.* **2017**, *4*, 790-803.
30
31
32

33 (44) Westphal, E.; Bechtold, I. H.; Gallardo, H. Synthesis and Optical/Thermal Behavior of
34
35 New Azo Photoisomerizable Discotic Liquid Crystals. *Macromolecules* **2010**, *43*, 1319-
36
37 1328.
38
39

40 (45) Peng, X.; Gao, H.; Xiao, Y.; Cheng, H.; Huang, F.; Cheng, X. Synthesis and Self-
41
42 Assembly of Photoresponsive and Luminescent Polycatenar Liquid Crystals Incorporating an
43
44 Azobenzene Unit Interconnecting Two 1,3,4-Thiadiazoles. *New J. Chem.* **2017**, *41*, 2004-
45
46 2012.
47
48
49
50
51
52
53
54
55
56
57
58
59
60

Table of Contents Graphic

